Metallocalix[4]arene Polymers for Gravimetric Detection of N- Nitrosodialkylamines

HHS Public Access

Author manuscript

J Am Chem Soc. Author manuscript; available in PMC 2022 December 01.

Published in final edited form as:

J Am Chem Soc. 2021 December 01; 143(47): 19809–19815. doi:10.1021/jacs.1c08739.

Metallocalix[4]arene Polymers for Gravimetric Detection of *N*–Nitrosodialkylamines

Ru-Qiang Lu,
Department of Chemistry, Massachusetts Institute of Technology, Cambridge, Massachusetts 02139, United States

Weize Yuan,
Department of Chemistry, Massachusetts Institute of Technology, Cambridge, Massachusetts 02139, United States

Robert G. Croy,
Department of Biological Engineering and Center for Environmental Health Sciences, Massachusetts Institute of Technology, Cambridge, Massachusetts 02139, United States

John M. Essigmann,
Department of Chemistry and Department of Biological Engineering and Center for Environmental Health Sciences, Massachusetts Institute of Technology, Cambridge, Massachusetts 02139, United States

Timothy M. Swager
Department of Chemistry and Department of Biological Engineering and Center for Environmental Health Sciences, Massachusetts Institute of Technology, Cambridge, Massachusetts 02139, United States

Abstract

N-Nitrosamines are found in food, drugs, air, water, and soil. They pose a significant risk to human health because of their carcinogenicity; consequently, materials that can be used to selectively and sensitively detect nitrosamines are needed. In this work, we designed and synthesized two polymers bearing calix[4]arene or 4-*tert*-butylcalix[4]arene tungsten−imido complexes (PCalixH and PCalixtBu) as *N*-nitrosodimethylamine (NDMA) receptors. The interaction between metallocalix[4]arene monomers/polymers and NDMA was confirmed by ^{1}H NMR and IR spectroscopy. Single-crystal X-ray analysis further revealed that the host−guest interaction is based on binding of the terminal oxygen of NDMA to tungsten within the calixarene cavity. Gravimetric detection of NDMA was performed on a quartz crystal microbalance (QCM) in air. Both polymers show responses to NDMA, with PCalixtBu exhibiting a low theoretical limit

Corresponding Author: Timothy M. Swager − Department of Chemistry and Department of Biological Engineering and Center for Environmental Health Sciences, Massachusetts Institute of Technology, Cambridge, Massachusetts 02139, United States; tswager@mit.edu.

Accession Codes

CCDC 2103918 contains the supplementary crystallographic data for this paper. These data can be obtained free of charge via www.ccdc.cam.ac.uk/data_request/cif, or by emailing data_request@ccdc.cam.ac.uk, or by contacting The Cambridge Crystallographic Data Centre, 12 Union Road, Cambridge CB2 1EZ, U.K.; fax: +44 1223 336033.

The authors declare no competing financial interest.

of detection of 5 ppb for NDMA. The sensor also shows high selectivity toward NDMA and moderate humidity tolerance. This work provides a sensitive sensor for detection of NDMA and also offers a class of new, selective, and efficient NDMA receptors for the future design of NDMA sensors and NDMA extraction materials.

Graphical Abstract

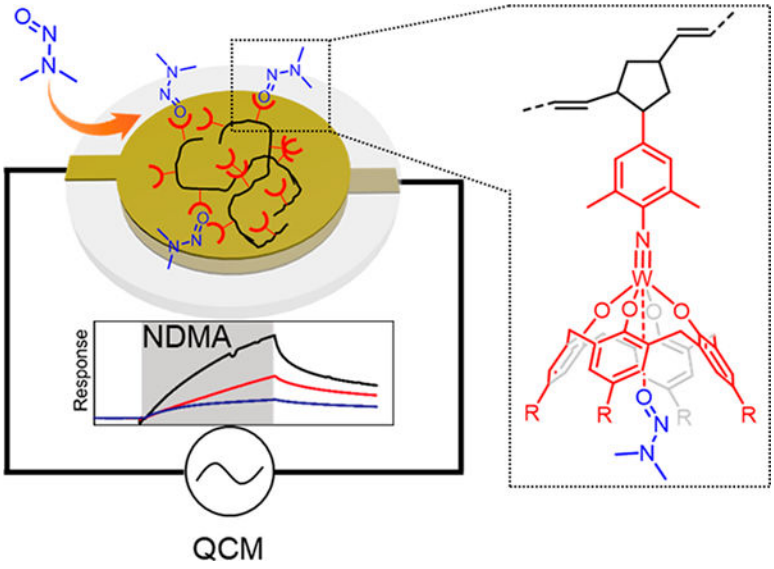

INTRODUCTION

N-Nitrosamines are organic compounds with chemical structures of $R_2N{-}N{=}O$. They are known carcinogenic species, and metabolic processes create diazonium ions that lead to mutagenic DNA damage by alkylation and in this way initiate cancer.[1–4] The need for environmental sensors is underscored by the recent report of the Massachusetts Department of Public Health's Bureau of Environmental to *N*-nitrosodimethylamine (NDMA) and childhood cancer in Wilmington, Massachusetts.[5] The International Agency for Research on Cancer has also classified NDMA as a group 2A carcinogen (probably carcinogenic to humans).[6] NDMA and other *N*-nitrosamines are unintentionally produced by disinfection of water containing organic amines using chlorinated chemicals[7] and the manufacture of medicines[8] as well as rubber and plastic.[9] For example, high levels of *N*-nitrosamines in air (0.1−380 $\mu g/m^3$) have been found in some rubber and tire factories.[10] NDMA is also found in some foods such as cured or smoked meats[11] and beers[12] as a result of their preparation.

To protect the public from the potential health hazards of these species, the development of simple and sensitive detection methods to monitor the concentration of *N*-nitrosamines is desired. Over the past decades, several simple and inexpensive methods have been developed to enable the detection of ppm to sub-ppb levels of NDMA.[4,13–17] These methods include chemiresistor sensors and photo/electrochemical spectroscopy. For example, chemiresistors for the selective detection of ppb levels of NDMA in air were created using a cobalt(III) tetraphenylporphyrin selector.[14] Anzenbacher and co-workers developed cucurbit[*n*]uril

(CB[*n*]) fluorescent probes that allowed the detection of NDMA in water.[13] Wen and co-workers achieved sub-ppb detection of NDMA and *N*-nitrosodiethylamine (NDEA) using a surface-enhanced Raman scattering technique.[16] These examples provide valuable platforms and strategies for nitrosamine detection. However, sensitive, simple, and cost-effective detection modalities of nitrosamines are still limited. The quartz crystal microbalance (QCM) is a sensitive acoustic sensing technique that can detect nanogram to microgram mass changes per unit area.[18–22] Acoustic sensors such as QCM and related surface acoustic wave devices provide fast, reliable, and real-time responses to analytes.[23–25] Combining the highly sensitive nature of QCMs and selectivity of a material toward nitrosamines provides a new approach to nitrosamine detection.

Innovations in materials science have opened the door for sensitive detection of nitrosamines. Currently, materials containing specifically designed receptors or selectors to interact with nitrosamines are rare. Calix[4]arenes are well-established supramolecular scaffolds, and derivatives have demonstrated binding of smaller molecules and ions.[26–31] The parent calix[4]arene structure is flexible, and the phenol subunits can rotate to form four possible conformations: cone, partial cone, 1,2-alternate, and 1,3-alternate. To rigidify the structure, Corazza et al. and we have applied a tungsten cap structure, Corazza et al. and we have applied a tungsten cap that enforces a cone structure to create a preorganized and highly restricted cavity.[32–35] Additionally, the five-coordinate metal center provides Lewis acidity within the cavity defined by the cone, which has high affinity for Lewis bases such as dimethylformamide and dimethyl sulfoxide.[33,34] The terminal oxygen of nitrosamines is partly negatively charged as a result of the zwitterionic resonance structure.[4] Therefore, we targeted tungsten-capped calix[4]arenes as nitrosamine receptors. Polymer materials usually have better film-forming properties than small molecules. The incorporation of tungsten-capped calix[4]arenes into polymers could facilitate the production of optimal coatings for QCM analysis.

Herein we report the design and synthesis of two polymers by ring-opening olefin metathesis polymerization (ROMP) of norbornyl monomers containing calix[4]arene or 4-*tert*-butylcalix[4]arene tungsten−imido complexes. The interaction between monomers and NDMA was revealed by ^{1}H NMR and single-crystal X-ray analyses. The tungsten-capped calix[4]arene binds NDMA through the interaction between the oxygen of NDMA and tungsten. Theoretical calculations revealed that the 4-*tert*-butylcalix[4]arene tungsten−imido complex shows stronger binding to NDMA than the calix[4]arene tungsten−imido complex. ^{1}H NMR and infrared (IR) spectra further confirmed that the ROMP polymers bearing tungsten-capped calix[4]arenes can also bind NDMA. The NDMA gravimetric detection capabilities of the polymers were evaluated using a QCM in air. The theoretical limit of detection of NDMA in air is about 5 ppb for PCalixtBu, which is exceptional for such a simple and inexpensive detection method. Furthermore, the sensor shows high selectivity toward NDMA and retains a high response to NDMA in humid air. Our work not only provides a sensitive sensor for detection of NDMA in air but also demonstrates new, selective, and efficient NDMA receptors for future designs of NDMA sensors and/or NDMA extraction materials.

RESULTS AND DISCUSSION

The synthesis of ROMP polymers is shown in Scheme 1. Calixarene monomer **2** was synthesized according to a known procedure,[36] and compound **1** was synthesized in a similar way. The ROMP reaction was catalyzed by the Grubbs third-generation catalyst, and the characterization of the polymers is summarized in Table 1. A molecular weight of 56.6 kDa was obtained for PCalixH, and that of PCalixtBu is 63.2 kDa. The two polymers exhibit good solubility in common solvents such as dichloromethane, tetrahydrofuran, chloroform, and toluene (solubility > 10 mg/mL). Both polymers show high decomposition temperatures (>405 °C with 5% weight loss under nitrogen; Figure S1).

The interaction of the two monomers with NDMA was confirmed by ^{1}H NMR spectroscopy, wherein a new set of peaks attributed to the corresponding complex arose upon addition of NDMA (Figures 1 and S2). ^{1}H−^{1}H nuclear Overhauser effect spectroscopy (NOESY) of the mixture of **1** and NDMA was performed (Figure S3b). Space correlations between protons H_a and H_b of bound NDMA and H_c and H_d of **1** were observed. The exchange of free and bound NDMA was also observed by ^{1}H−^{1}H exchange spectroscopy (EXSY) (Figure S3c). These results confirm that the peaks at 0.67 and 2.14 ppm are from bound NDMA. The binding ratio was determined to be 1:1 for both monomers and NDMA. The binding constants for the two monomers and NDMA are difficult to accurately determine because of competition for the binding site by residual water in the solvents. Nevertheless, the binding between the monomers and water is weaker than that between the monomers and NDMA, as will be discussed later. Crystals of model compound **3** and NDMA obtained by slow evaporation of a dichloromethane/hexane solution of NDMA and **3** (Table S1) were suitable for X-ray structure determination. NDMA in the cocrystal is disordered over two positions (Figure 2a). The cavity of **3** perfectly fits an NDMA molecule. As expected, each host molecule binds one NDMA molecule through a Lewis acid−base interaction between the tungsten and the terminal oxygen of the *N*-nitrosamine. The distances between the W atom and the oxygen atoms of the two disordered NDMA molecules are 2.264 and 2.245 Å, respectively, which are much shorter than the sum of the van der Waals radii of W (~2.1 Å) and O (~1.4 Å) atoms.[37] This result indicates the strong interaction between the metallocalixarene and NDMA. Upon binding, the bond lengths of NDMA change slightly: the N−N bond shortens from 1.320 to 1.282 Å, and the N=O bond elongates from 1.260 to 1.286 Å (Figure 2b).[38] The results suggest a significant contribution of the dipolar resonance structure of NDMA (Figure 2c) in the complex.

To further reveal the binding properties of the monomers and NDMA, density functional theory (DFT) calculations were performed on the model molecules. According to the simulated molecular model, the cavity of **4** accommodates NDMA despite the presence of the bulky *t*-Bu groups (Figure S14b). The binding energies for complexation of NDMA were estimated to be 32.9 kcal/mol for **3** and 34.8 kcal/mol for **4** (Figure S14). The higher binding energy between **4** and NDMA may result from the van der Waals forces between the methyl groups of NDMA and the *t*Bu groups of **4**. The binding energies between **3** or **4** and a single water molecule are 30.6 and 31.1 kcal/mol, respectively, which are lower than the values for NDMA. These theoretical results reveal that the binding of the metallocalix[4]arenes with NDMA is stronger than that with water. Additionally, the bond length changes for

bound NDMA are consistent with those in the single crystal (Figure 2b). For the **3**−NDMA complex as an example, the N−N bond shortens from 1.328 to 1.277 Å, and the N=O bond elongates from 1.223 to 1.254 Å.

The strong binding between the metallocalixarene monomers and NDMA is expected to be conserved in the polymers. We performed ^{1}H NMR and IR analyses, which confirmed this hypothesis. For PCalixH, precipitation was observed when NDMA was added to the polymer solution in CD_2Cl_2, which prevented collection of ^{1}H NMR signals for the polymer (Figure S4). A new IR peak at 1316 cm^{-1} arose when PCalixH was mixed with NDMA (Figure 3a). This peak is attributed to the overlapping ν_{N-N} and $\nu_{N=O}$ stretching vibrations of bound NDMA, and this result is consistent with those for other *N*-nitrosamine−metal complexes.[39–42] Additionally, the IR spectrum of the PCalixH−NDMA complex inherits almost all of the characteristic peaks of PCalixH, indicating that the precipitation of PCalixH with NDMA is not the result of decomposition. The decrease in solubility of PCalixH is physical in nature, and the reason remains unknown. The interaction between PCalixtBu and NDMA was confirmed by ^{1}H NMR spectroscopy, where two new broad peaks at 0.71 and 2.03 ppm attributed to the PCalixtBu−NDMA complex was observed (Figure S5). IR spectra further confirmed the binding. A peak at 1325 cm^{-1} attributed to the overlapping ν_{N-N} and $\nu_{N=O}$ stretching vibrations of bound NDMA was observed for the complex (Figure 3b).

We evaluated the NDMA sensing performance of the two polymers using a QCM. The sensing setups are shown in Figure S6. The polymers were drop-cast on QCM resonators (Figure S7). The response was defined as $(f_1 - f)/(f_0 - f_1) \times 100\%$, where f_0 is the fundamental oscillation frequency of a QCM quartz crystal, f_1 is the frequency after material deposition on that crystal and f is the frequency of the film coated crystal measured during the sensing experiment. All of the sensing traces were recorded in air (relative humidity (RH) ≈ 5%) with an exposure time of 6 min. The responses of PCalixH and PCalixtBu to 5 ppm NDMA were 0.134 ± 0.013% and 0.595 ± 0.178%, respectively (Figures 4a and S8). The higher sensitivity of PCalixtBu to NDMA is consistent with the higher binding energy of NDMA with the model molecule **4** than that with **3**. Furthermore, the Brunauer−Emmett−Teller (BET) surface area of PCalixtBu is 91 ± 24 m^2/g, which is higher than that of PCalixH (32 ± 16 m^2/g) (Table 1 and Figure S9). A higher surface area can promote the interaction between the metallocalix[4]arene moiety and NDMA. The pore size distributions of both polymers are broad, ranging from 1 nm to >25 nm (Figure S9b,d). We further evaluated the NDMA sensing performance of PCalixtBu because of its higher response to NDMA. The response of PCalixtBu to NDMA changes linearly with the NDMA concentration from 100 ppb to 10 ppm (Figure 4c). The limit of detection was calculated to be about 5 ppb (see the Supporting Information for details).[43,44] The value is similar to the reported performance of simple and inexpensive NDMA sensors in air.[14]

The sensor based on PCalixtBu also showed high selectivity toward NDMA and retained a high response to NDMA in humid air. The responses of PCalixtBu toward 50−150 ppm levels of other volatile organic compounds (VOCs), including hexane, benzene, tetrahydrofuran (THF), ethyl ether (Et_2O), methanol, ethanol, acetone, ethyl acetate (EA), acetonitrile, triethylamine (Et_3N), and the nitrosamine precursor diethylamine (DEA),[45–49] were much lower than the response to 10 ppm NDMA (Figures 4d and S10). The

concentrations of common VOCs in ambient air are usually lower than 100 ppb.[50–52] We measured the responses of PCalixtBu to some representative VOCs at 100 ppb. PCalixtBu did not show any observable responses (Figure S11). In comparison, the response of PCalixtBu to 100 ppb NDMA was 0.026 ± 0.004% (Figure 4b). This indicates that the selectivity of PCalixtBu to NDMA remains high at a low concentration. In some rubber and tire factories, the concentration of NDMA was found to be as high as 140 $\mu g/m^3$ (1 $\mu g/m^3$ NDMA = 3 ppb NDMA).[10] The PCalixtBu-based sensor could potentially be used in monitoring the NDMA concentration in those factories that may emit a high concentration of NDMA. Extremely high concentrations of interfering VOCs may influence the determination of NDMA concentration. In this case, a sensor array with the PCalixtBu-based sensor and other complementary recognition elements could be incorporated to differentiate VOCs and determine the concentration of NDMA.

PCalixtBu is also responsive to larger *N*-nitrosodialkylamines such as NDEA and *N*-nitrosodibutylamine (NDBA), but the responses are lower than that to NDMA (Figure S12a). This may result from the larger size of NDEA and NDBA, which may prevent them from optimally interacting with the Lewis acidic tungsten center within the cavity of the metallocalix[4]arene. Size-match effects can also be used to explain the higher response of PCalixtBu to DEA than to Et_3N on the basis of the smaller size of DEA. Overall, the Lewis acidic metal center and the restricted cavity of the tungsten-capped calix[4]arene are the keys to achieving such high selectivity. The response to NDMA decreases from 1.05 to 0.42 with an increase in relative humidity from ~5% to ~78% (Figure S12b). The response in the air with a high RH of 78% is still high, revealing the promising applications of the sensor in the real world.

CONCLUSION

We have developed a new class of nitrosamine receptors based on calix[4]arene tungsten−imido complexes. The interaction between the calix[4]arene tungsten−imido complexes and NDMA was revealed by ^1H NMR, IR, and single-crystal X-ray analyses. Gravimetric detection of *N*-nitrosodialkylamines was achieved using a QCM. The polymers based on the receptors show high sensitivity and selectivity toward NDMA. A theoretical limit of detection of 5 ppb for NDMA was achieved in air. The sensor also retains relatively high sensitivity to NDMA in humid air. This work provides a new, fast, and cost-effective sensing modality to detect NDMA in air using the QCM gas sensor. The materials reported here can also be used broadly in the design of materials for detection and extraction of nitrosamines.

Supplementary Material

Refer to Web version on PubMed Central for supplementary material.

ACKNOWLEDGMENTS

We are thankful for computational resources kindly provided by the Massachusetts Green High-Performance Computing Center (MGHPCC) C3DDB cluster. We thank Mohanraja Kumar at DCIF of MIT, Prof. Desiree Plata, Jessica Beard, and Shao-Xiong Lennon Luo for valuable discussions.

Funding

This work was supported by the National Institute of Environmental Health Sciences Superfund Basic Research Program, National Institutes of Health (P42 ES027707).

REFERENCES

(1). Yamazaki H; Inui Y; Yun C-H; Guengerich FP; Shimada T Cytochrome P450 2E1 and 2A6 enzymes as major catalysts for metabolic activation of N-nitrosodialkylamines and tobacco-related nitrosamines in human liver microsomes. Carcinogenesis 1992, 13, 1789–1794. [PubMed: 1423839]

(2). Tricker AR; Preussmann R Carcinogenic N-nitrosamines in the diet: occurrence, formation, mechanisms and carcinogenic potential. Mutat. Res., Genet. Toxicol. Test 1991, 259, 277–289.

(3). Hecht SS Tobacco carcinogens, their biomarkers and tobacco induced cancer. Nat. Rev. Cancer 2003, 3, 733–744. [PubMed: 14570033]

(4). Beard JC; Swager TM An Organic Chemist's Guide to N-Nitrosamines: Their Structure, Reactivity, and Role as Contaminants. J. Org. Chem 2021, 86, 2037–2057. [PubMed: 33474939]

(5). The Wilmington Childhood Cancer Study: An Epidemiologic Investigation of Childhood Cancer from 1990−2000; Bureau of Environmental Health, Massachusetts Department of Public Health, 2021; https://www.mass.gov/doc/full-study-report/download (accessed 2021-08-01).

(6). International Agency for Research on Cancer. Agents Classified by the IARC Monographs, Volumes 1−129 https://monographs.iarc.who.int/list-of-classifications (accessed 2021-08-01).

(7). Mitch WA; Sedlak DL Formation of N-Nitrosodimethylamine (NDMA) from Dimethylamine during Chlorination. Environ. Sci. Technol 2002, 36, 588–595. [PubMed: 11878371]

(8). Control of Nitrosamine Impurities in Human Drugs: Guidance for Industry; U.S. Food and Drug Administration, 2020.

(9). OSHA Hazard Information Bulletins: N-Nitroso Compounds in Industry; Occupational Safety and Health Administration, U.S. Department of Labor, 1990.

(10). Spiegelhalder B; Preussmann R Occupational nitrosamine exposure. 1. Rubber and tyre industry. Carcinogenesis 1983, 4, 1147–1152. [PubMed: 6883637]

(11). Dich J; Järvinen R; Knekt P; Penttilä PL Dietary intakes of nitrate, nitrite and NDMA in the Finnish mobile clinic health examination survey. Food Addit. Contam 1996, 13, 541–552. [PubMed: 8799716]

(12). Bellec G; Cauvin JM; Salaun MC; Le Calvé K; Dréano Y; Gouérou H; Ménez JF; Berthou F Analysis of N-nitrosamines by high-performance liquid chromatography with post-column photohydrolysis and colorimetric detection. J. Chromatogr. A 1996, 727, 83–92. [PubMed: 8900963]

(13). Minami T; Esipenko NA; Zhang B; Kozelkova ME; Isaacs L; Nishiyabu R; Kubo Y; Anzenbacher P Supramolecular Sensor for Cancer-Associated Nitrosamines. J. Am. Chem. Soc. 2012, 134, 20021–20024. [PubMed: 23194337]

(14). He M; Croy RG; Essigmann JM; Swager TM Chemiresistive Carbon Nanotube Sensors for N-Nitrosodialkylamines. ACS Sens 2019, 4, 2819–2824. [PubMed: 31573183]

(15). Cetó X; Saint CP; Chow CWK; Voelcker NH; Prieto-Simón B Electrochemical detection of N-nitrosodimethylamine using a molecular imprinted polymer. Sens. Actuators, B 2016, 237, 613–620.

(16). Lin C-H; Wang P-H; Wang T-H; Yang L-J; Wen T-C The surface-enhanced Raman scattering detection of N-nitrosodimethylamine and N-nitrosodiethylamine via gold nanorod arrays with a chemical linkage of zwitterionic copolymer. Nanoscale 2020, 12, 1075–1082. [PubMed: 31845933]

(17). Fiddler W The occurrence and determination of N-Nitroso compounds. Toxicol. Appl. Pharmacol 1975, 31, 352–360. [PubMed: 1096365]

(18). Huang R; Yi P; Tang Y Probing the interactions of organic molecules, nanomaterials, and microbes with solid surfaces using quartz crystal microbalances: methodology, advantages, and limitations. Environ. Sci. Process. Impacts 2017, 19, 793–811. [PubMed: 28488712]

(19). Applications of Piezoelectric Quartz Crystal Microbalances; Lu C, Czanderna AW, Eds.; Methods and Phenomena 7; Elsevier Science Publishers B.V.: Amsterdam, 1984.

(20). Cady WG Piezoelectricity: An Introduction to the Theory and Applications of Electromechanical Phenomena; Dover Publications: New York, 1964.

(21). Ward MD; Buttry DA In Situ Interfacial Mass Detection with Piezoelectric Transducers. Science 1990, 249, 1000. [PubMed: 17789608]

(22). Nanoscience Instruments. Quartz Crystal Microbalance (QCM) https://www.nanoscience.com/techniques/quartz-crystal-microbalance/#theory (accessed 2021-08-01).

(23). Cooper MA; Singleton VT A survey of the 2001 to 2005 quartz crystal microbalance biosensor literature: applications of acoustic physics to the analysis of biomolecular interactions. J. Mol. Recognit 2007, 20, 154–184. [PubMed: 17582799]

(24). Becker B; Cooper MA A survey of the 2006−2009 quartz crystal microbalance biosensor literature. J. Mol. Recognit 2011, 24, 754–787. [PubMed: 21812051]

(25). Dixon MC Quartz crystal microbalance with dissipation monitoring: enabling real-time characterization of biological materials and their interactions. J. Biomol. Tech 2008, 19, 151–158. [PubMed: 19137101]

(26). Zhou Y; Jie K; Zhao R; Huang F Supramolecular-Macrocycle-Based Crystalline Organic Materials. Adv. Mater 2020, 32, 1904824.

(27). Mutihac L; Lee JH; Kim JS; Vicens J Recognition of amino acids by functionalized calixarenes. Chem. Soc. Rev 2011, 40, 2777–2796. [PubMed: 21321724]

(28). Kumar R; Sharma A; Singh H; Suating P; Kim HS; Sunwoo K; Shim I; Gibb BC; Kim JS Revisiting Fluorescent Calixarenes: From Molecular Sensors to Smart Materials. Chem. Rev 2019, 119, 9657–9721. [PubMed: 31306015]

(29). Gutsche CD The calixarenes. Top. Curr. Chem 1984, 123, 1–47.

(30). Gutsche CD Calixarenes. Acc. Chem. Res 1983, 16, 161–70.

(31). Diamond D; McKervey MA Calixarene-based sensing agents. Chem. Soc. Rev 1996, 25, 15–24.

(32). Corazza F; Floriani C; Chiesi-Villa A; Rizzoli C Mononuclear tungsten(VI) calix[4]arene complexes. Inorg. Chem 1991, 30, 4465–4468.

(33). Vigalok A; Swager TM Conducting Polymers of Tungsten(VI)−Oxo Calixarene: Intercalation of Neutral Organic Guests. Adv. Mater 2002, 14, 368–371.

(34). Swager TM; Xu B Liquid crystalline calixarenes. J. Inclusion Phenom. Mol. Recognit. Chem 1994, 19, 389–398.

(35). Zhao Y; Swager TM Detection and Differentiation of Neutral Organic Compounds by 19F NMR with a Tungsten Calix[4]arene Imido Complex. J. Am. Chem. Soc 2013, 135, 18770–18773. [PubMed: 24299149]

(36). Zhao Y; Swager TM Functionalized Metalated Cavitands via Imidation and Late-Stage Elaboration. Eur. J. Org. Chem 2015, 2015, 4593–4597.

(37). Batsanov SS Van der Waals Radii of Elements. Inorg. Mater 2001, 37, 871–885.

(38). Krebs B; Mandt J Kristallstruktur des N-Nitrosodimethylamins. Chem. Ber 1975, 108, 1130–1137.

(39). Chen L; Yi G-B; Wang L-S; Dharmawardana UR; Dart AC; Khan MA; Richter-Addo GB Synthesis, Characterization, and Molecular Structures of Diethylnitrosamine Metalloporphyrin Complexes of Iron, Ruthenium, and Osmium. Inorg. Chem 1998, 37, 4677–4688. [PubMed: 11670621]

(40). Xu N; Goodrich LE; Lehnert N; Powell DR; Richter-Addo GB Five- and Six-Coordinate Adducts of Nitrosamines with Ferric Porphyrins: Structural Models for the Type II Interactions of Nitrosamines with Ferric Cytochrome P450. Inorg. Chem 2010, 49, 4405–4419. [PubMed: 20392126]

(41). Yi G-B; Khan MA; Richter-Addo GB The First Metalloporphyrin Nitrosamine Complex: Bis(diethylnitrosamine)-(meso-tetraphenylporphyrinato)iron(III) perchlorate. J. Am. Chem. Soc 1995, 117, 7850–7851.

(42). Lee J; Chen L; West AH; Richter-Addo GB Interactions of Organic Nitroso Compounds with Metals. Chem. Rev 2002, 102, 1019–1066. [PubMed: 11942786]

(43). Li J; Lu Y; Ye Q; Cinke M; Han J; Meyyappan M Carbon Nanotube Sensors for Gas and Organic Vapor Detection. Nano Lett 2003, 3, 929–933.

(44). Currie LA Nomenclature in evaluation of analytical methods including detection and quantification capabilities (IUPAC Recommendations 1995). Pure Appl. Chem 1995, 67, 1699–1723.

(45). Shah AD; Mitch WA Halonitroalkanes, Halonitriles, Haloamides, and N-Nitrosamines: A Critical Review of Nitrogenous Disinfection Byproduct Formation Pathways. Environ. Sci. Technol 2012, 46, 119–131. [PubMed: 22112205]

(46). Chen Z; Valentine RL Modeling the Formation of N-Nitrosodimethylamine (NDMA) from the Reaction of Natural Organic Matter (NOM) with Monochloramine. Environ. Sci. Technol 2006, 40, 7290–7297. [PubMed: 17180980]

(47). Le Roux J; Gallard H; Croué J-P Chloramination of nitrogenous contaminants (pharmaceuticals and pesticides): NDMA and halogenated DBPs formation. Water Res 2011, 45, 3164–3174. [PubMed: 21496861]

(48). Spahr S; Cirpka OA; von Gunten U; Hofstetter TB Formation of N-Nitrosodimethylamine during Chloramination of Secondary and Tertiary Amines: Role of Molecular Oxygen and Radical Intermediates. Environ. Sci. Technol 2017, 51, 280–290. [PubMed: 27958701]

(49). Schreiber IM; Mitch WA Nitrosamine Formation Pathway Revisited: The Importance of Chloramine Speciation and Dissolved Oxygen. Environ. Sci. Technol 2006, 40, 6007–6014. [PubMed: 17051792]

(50). Montero-Montoya R; López-Vargas R; Arellano-Aguilar O Volatile organic compounds in air: sources, distribution, exposure and associated illnesses in children. Ann. Glob. Health 2018, 84, 225. [PubMed: 30873816]

(51). Brown SK; Sim MR; Abramson MJ; Gray CN Concentrations of Volatile Organic Compounds in Indoor Air – A Review. Indoor Air 1994, 4, 123–134.

(52). Mohamed MF; Kang D; Aneja VP Volatile organic compounds in some urban locations in United States. Chemosphere 2002, 47, 863–882. [PubMed: 12079081]

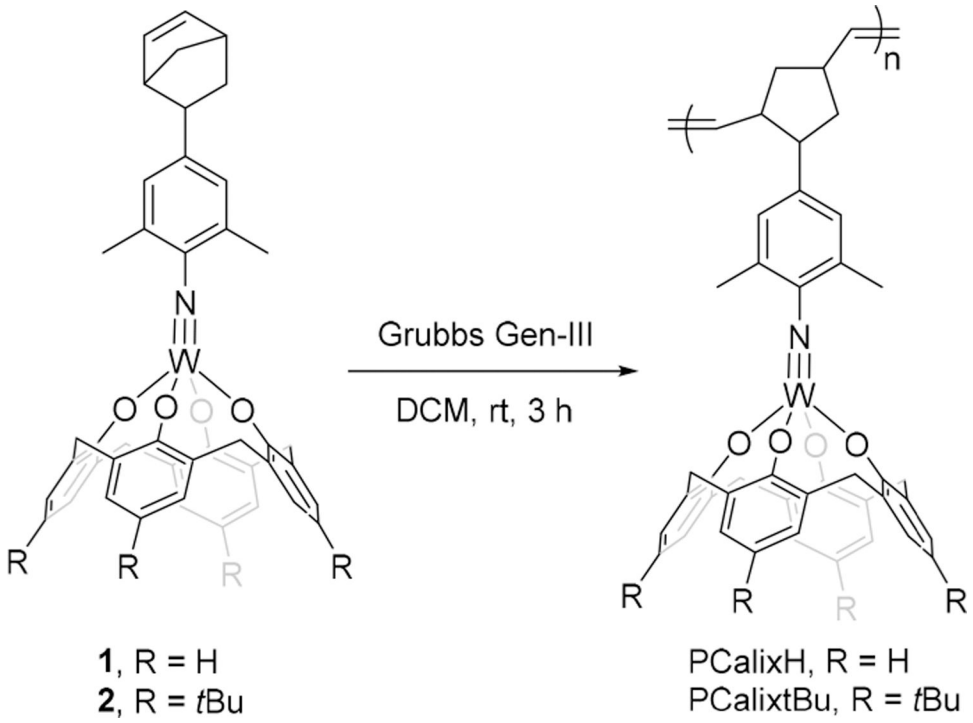

Scheme 1.
Synthesis of ROMP Polymers Bearing Tungsten-Capped Calix[4]arenes

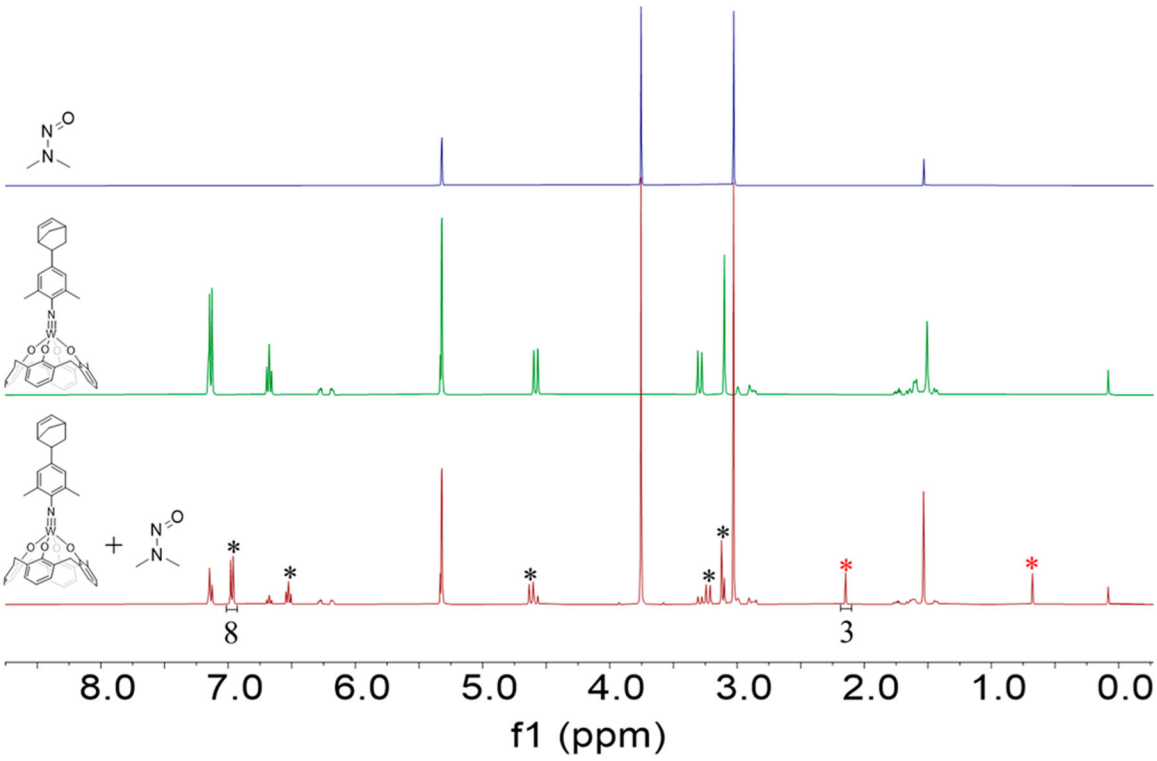

Figure 1.

^{1}H NMR spectra of NDMA, **1**, and their mixture in CD_2Cl_2. Signals from the **1**−NDMA complex are marked with black and red stars to indicate the resonances from **1** and NDMA, respectively.

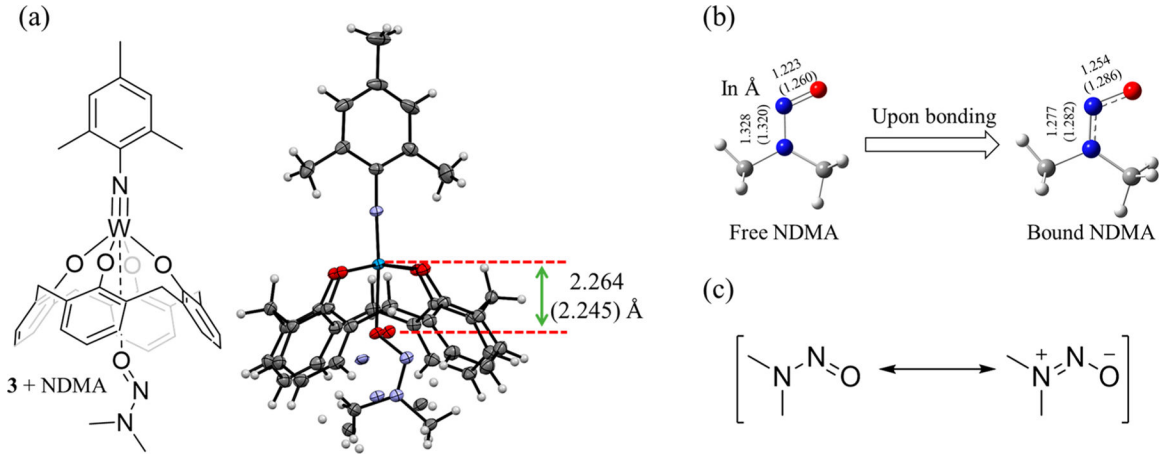

Figure 2.

(a) Cocrystal structure of model molecule **3** and NDMA. Thermal displacement ellipsoids are shown at 50% probability (carbon, gray; hydrogen, white; oxygen, red; nitrogen, purple; tungsten, cyan). (b) Selected bond lengths (in Å) of free NDMA and bound NDMA from single-crystal data (in parentheses) and theoretical calculations for the **3**−NDMA complex. (c) Resonance structures of NDMA.

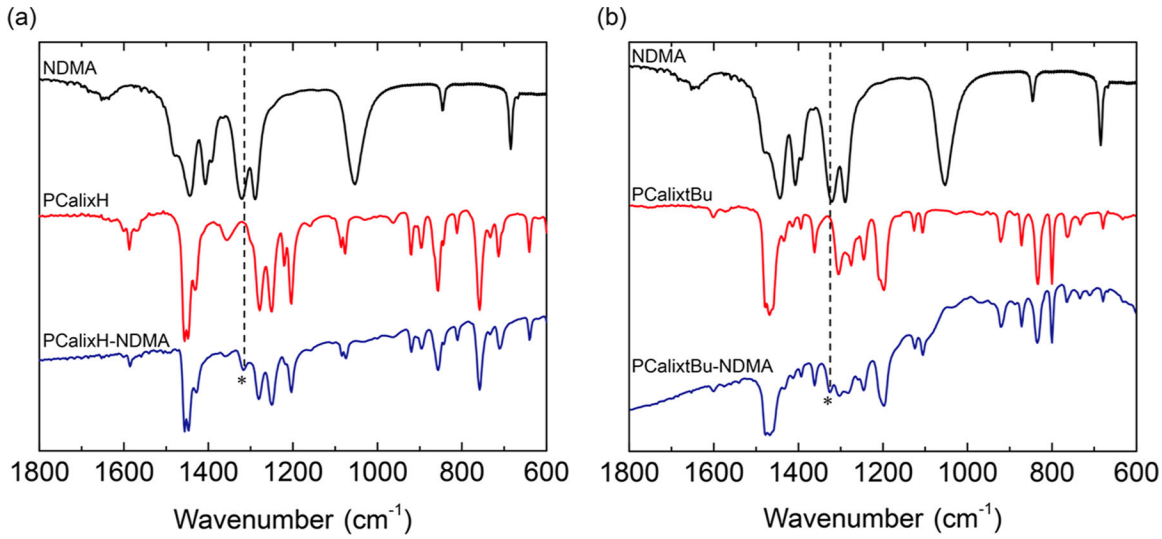

Figure 3.

IR spectra of (a) NDMA, PCalixH, and their complex and (b) NDMA, PCalixtBu, and their complex in the solid states. The complexes were prepared by mixing ROMP polymers with NDMA in CH_2Cl_2. The IR spectral data for NDMA were taken from ref 14.

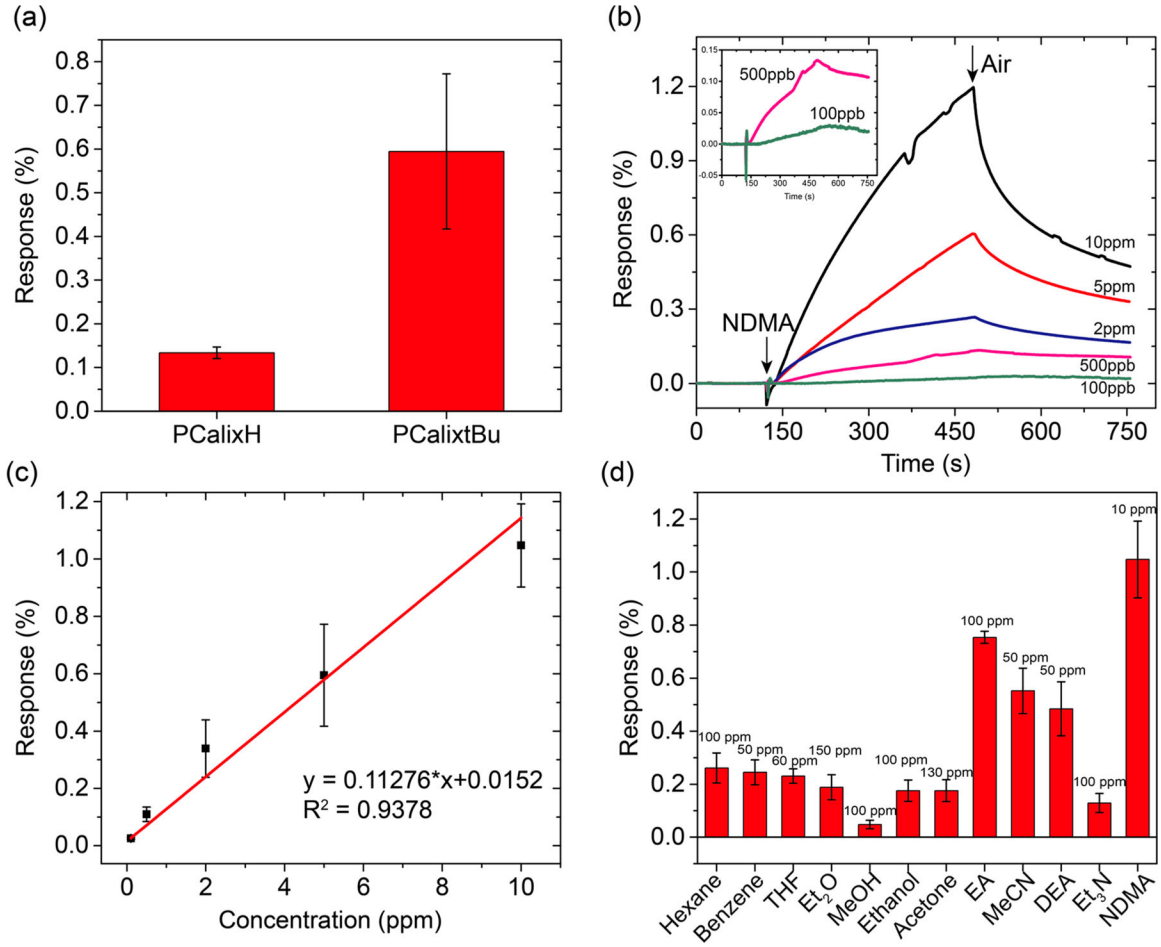

Figure 4.

(a) Response of PCalixH and PCalixtBu to NDMA (5 ppm). (b) Sensing traces of PCalixtBu with NDMA concentrations from 100 ppb to 10 ppm (third overtone). (c) Linear fit of the concentration-dependent response of PCalixtBu. (d) Response of PCalixtBu to VOCs. All of the sensing experiments were performed in air with a relative humidity of ~5%. The exposure time was 6 min. The error bars were calculated from three independent measurements.

Table 1.

Characterization of ROMP Polymers

polymer	M_n (kDa)	PDI	T_d (°C)	BET surface area (m^2/g)
PCalixH	56.6	1.26	425	32 ± 16
PCalixtBu	63.2	1.14	405	91 ± 24